

A PTAL-miR-101-FN1 Axis Promotes EMT and Invasion-Metastasis in Serous Ovarian Cancer

Haihai Liang,^{1,2,4} Mengxue Yu,^{1,4} Rui Yang,^{1,4} Lu Zhang,^{1,2} Lijia Zhang,¹ Di Zhu,¹ Hongwei Luo,¹ Yaozhen Hong,¹ Tong Yu,^{1,2} Jian Sun,^{1,2} Hongli Shan,^{1,2} and Yunyan Gu³

¹Department of Pharmacology (State-Province Key Laboratories of Biomedicine-Pharmaceutics of China, Key Laboratory of Cardiovascular Research, Ministry of Education), College of Pharmacy, Harbin Medical University, Harbin, Heilongjiang 150081, P.R. China; ²Translational Medicine Research and Cooperation Center of Northern China, Heilongjiang Academy of Medical Sciences, Harbin Medical University, Harbin, Heilongjiang 150081, P.R. China; ³Department of Systems Biology, College of Bioinformatics Science and Technology, Harbin Medical University, Harbin, Heilongjiang 150081, P.R. China

Long non-coding RNAs (lncRNAs) play vital roles in the metastasis and invasion of cancer cells. Systematic analysis of ovarian cancer (OvCa) expression profiles suggests that deregulation of lncRNA AC004988.1, designated promoting transition-associated lncRNA (PTAL), is involved in OvCa progression. However, the underlying mechanism of PTAL in OvCa remains unknown. In this study, we showed that PTAL was significantly upregulated in mesenchymal subtype samples compared with epithelial subtype samples from TCGA serous OvCa datasets. PTAL expression was positively correlated with the expression of fibronectin1 (FN1), whereas PTAL and FN1 were negatively correlated with miR-101 expression in the mesenchymal OvCa samples. In addition, knockdown of PTAL inhibited cell migration and invasion and blunted the progression of metastasis *in vitro*. Meanwhile, knockdown of PTAL increased the expression of miR-101 and subsequently inhibited the expression of FN1. Importantly, PTAL positively regulated the expression of FN1 through sponging of miR-101 and promoted OvCa cell metastasis by regulating epithelial-mesenchymal transition. Overall, our study demonstrates the role of PTAL as a miRNA sponge in OvCa and suggests that PTAL may be a potential target for preventing OvCa metastasis.

INTRODUCTION

Ovarian cancer (OvCa) is a malignancy with high incidence and high mortality rate in females.¹ The high rate of lethality from OvCa is primarily due to the advanced stage of disease at the time of diagnosis,^{2,3} and the poor prognosis of OvCa results from the invasion or metastasis of OvCa cells to other parts of the body.⁴ Evidence indicates that the ability of OvCa cells to invade and metastasize is enhanced through the loss of epithelial features and the gain of a mesenchymal phenotype, a process known as epithelial-to-mesenchymal transition (EMT).³ Low E-cadherin/Zo-1 expression and high vimentin/fibronectin 1 (FN1) expression are the characteristics of EMT. EMT is mediated by regulatory factors, such as transcription factors (TFs), microRNA (miRNA), and long non-coding RNA (lncRNA) at the transcriptional and post-transcriptional levels.⁵⁻⁷ lncRNAs, non-cod-

ing RNAs longer than 200 nucleotides, are emerging as new players in the cancer paradigm, demonstrating potential roles in both oncogenic and tumor-suppressive pathways.⁸ lncRNAs have been reported to play crucial regulatory roles in various cancers, such as lung cancer,⁹ breast cancer¹⁰ and OvCa.^{11,12} The lncRNA CYTOR is shown to be upregulated in colorectal cancer and associated with poor prognosis, promoting proliferation and metastasis by forming a complex with nucleolin (NCL) and Sam68.¹³ Moreover, some lncRNAs are thought to mediate the EMT process during the progression of carcinogenesis.^{14,15} For example, lncRNA-PNUTS serves as a competitive sponge for miR-205 during EMT in breast cancer,¹⁶ and lncRNA MEG3 plays an important role in lung cancer cell lines by regulating the EMT process through modulation of PRC2 recruitment and histone H3 methylation.¹⁷ However, the contribution of lncRNAs to EMT in OvCa is poorly understood.

To better characterize EMT in OvCa, we performed an integrated analysis of high-throughput OvCa data from several platforms, including mRNA, miRNA, and lncRNA expression profiles. We found that lncRNA AC004988.1, which was designated promoting transition-associated lncRNA (PTAL) in this study, and miR-101(miR-101-3p) were significantly differentially expressed in mesenchymal OvCa samples compared with epithelium OvCa samples, and we found a significant negative correlation between PTAL and miR-101 in mesenchymal OvCa samples. Although miR-101 has been confirmed to be involved in the regulation of invasion and migration in several cancer types, such as bladder cancer and hepatocellular carcinoma,^{18,19} the biological role and underlying molecular mechanism of miR-101 in OvCa remains largely unknown.

Received 25 December 2018; accepted 3 December 2019;
<https://doi.org/10.1016/j.omto.2019.12.002>.

⁴These authors contributed equally to this work.

Correspondence: Yunyan Gu, Department of Systems Biology, College of Bioinformatics Science and Technology, Harbin Medical University, Harbin, Heilongjiang 150081, P.R. China.

E-mail: guyunyan@ems.hrbmu.edu.cn



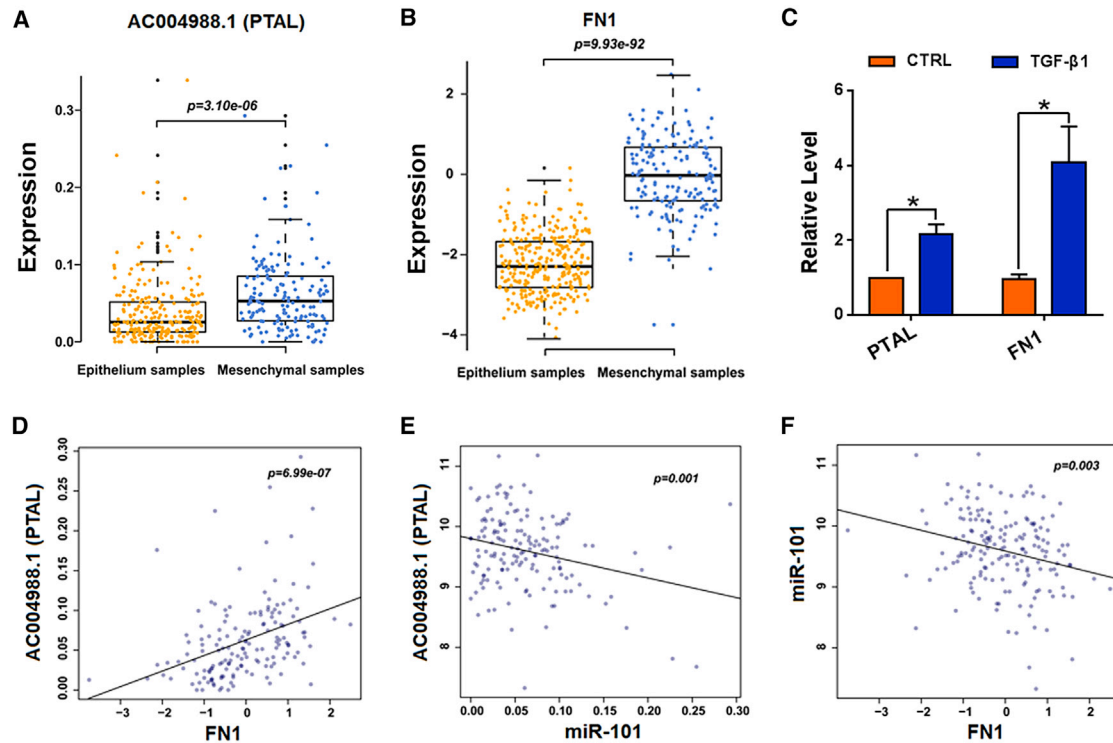


Figure 1. The PTAL-miR-101-FN1 Axis Is Dysregulated in OvCa

(A) PTAL is significantly upregulated in mesenchymal OvCa samples compared with epithelial OvCa samples in the TCGA dataset. (B) FN1 is significantly upregulated in mesenchymal OvCa samples compared with epithelial OvCa samples in the TCGA dataset. (C) Upregulation of PTAL and FN1 in SKOV3 cells after treatment with TGF- β 1. $n = 6$; * $p < 0.05$. (D) PTAL expression is positively correlated with FN1 expression in the TCGA dataset. (E) PTAL expression is negatively correlated with miR-101 expression in the TCGA dataset. (F) FN1 expression is negatively correlated with miR-101 expression in the TCGA dataset.

Moreover, increasing evidence has shown that lncRNAs can function as a natural miRNA sponge. Thus, we focus on investigating the interaction between PTAL and miR-101 in OvCa.

In this study, we found that PTAL was upregulated in OvCa and explored the effect of PTAL on the phenotype of OvCa cells both *in vitro* and *in vivo*. Furthermore, we revealed that PTAL played an oncogenic role in OvCa pathogenesis, within which PTAL functioned as a miRNA sponge to positively regulate the expression of FN1 through sponging of miR-101. Overall, the observations presented here elucidate the role of PTAL as a key regulator of metastasis of OvCa cells and suggest the possibility of PTAL as a marker of OvCa metastasis.

RESULTS

PTAL-miR-101-FN1 Axis Is Dysregulated in OvCa Samples

According to the competing endogenous RNA (ceRNA) network for integrated mesenchymal (iM) OvCa, which was constructed in our previous work,²⁰ we identified lncRNA AC004988.1, miR-101, and FN1 as being significantly differentially expressed in iM OvCa samples ($p < 0.05$). As an extracellular matrix glycoprotein, FN1 is involved in cellular adhesion, migration, and tumor progression in

multiple tumor types.^{21–23} In addition, it has been reported that miR-101 is a key miRNA that regulates the largest number of iM-related genes.^{3,24} The functional role and molecular mechanism of AC004988.1 in OvCa is still unknown. We found that lncRNA AC004988.1 and FN1 were significantly overexpressed in the iM OvCa samples from The Cancer Genome Atlas (TCGA) dataset ($p = 3.10 \times 10^{-6}$ for AC004988.1, $p = 9.93 \times 10^{-92}$ for FN1, *t* test; Figures 1A and 1B). Furthermore, lncRNA AC004988.1 and FN1 were also upregulated in transforming growth factor β 1 (TGF- β 1)-treated SKOV3 cells (Figure 1C). Moreover, FN1 expression was positively correlated with the expression level of lncRNA AC004988.1 (ENST00000415237.1) in the iM OvCa samples in the mesenchymal-related ceRNA network ($p = 6.99 \times 10^{-7}$, Pearson's correlation test; Figure 1D). Nevertheless, hsa-miR-101 expression was negatively correlated with the expression level of lncRNA AC004988.1 ($p = 0.001$, Pearson's correlation test; Figure 1E), and FN1 expression was also negatively correlated with the expression level of hsa-miR-101 ($p = 0.003$, Pearson's correlation test; Figure 1F). Thus, we hypothesized that lncRNA AC004988.1 positively regulated the expression of FN1 by competitively sponging miR-101 and played an oncogenic role in OvCa progression. For convenience, we refer to AC004988.1 as PTAL in this study.

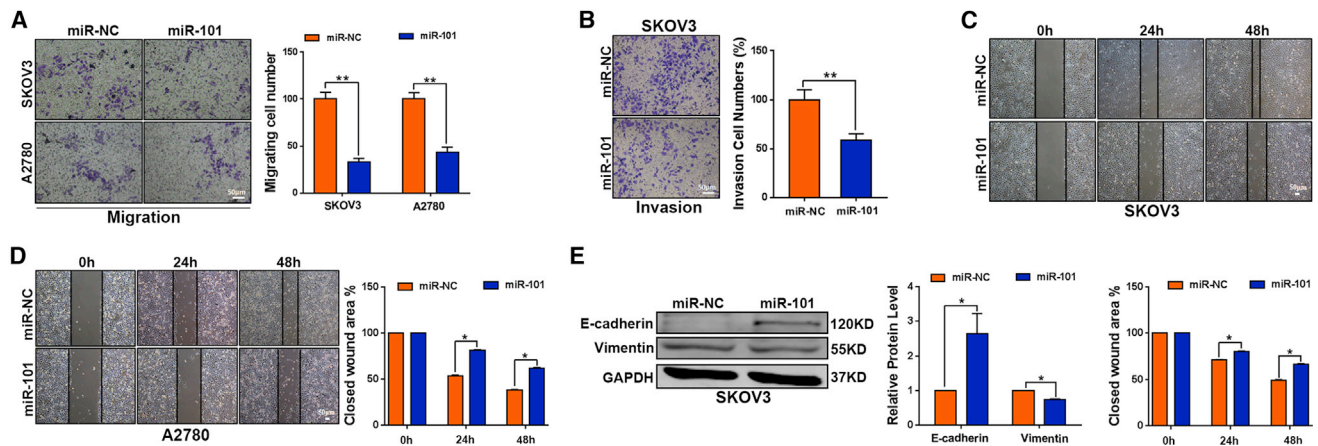


Figure 2. miR-101 Inhibits the Migration and Invasion of OvCa Cells

SKOV3 cells and A2780 cells were transfected with miR-101. (A) Representative images of the migration of SKOV3 and A2780 cells. Cells were counted for the corresponding assays in at least four random microscope fields ($\times 100$ magnification). Cell migration is expressed as a percentage of the control values. (B) Representative images of the invasion of SKOV3 cells. Cells were counted for the corresponding assays in at least four random microscope fields ($\times 100$ magnification). Cell invasion is expressed as a percentage of the control values. (C) Representative images from wound-healing assays of SKOV3 cells ($\times 40$ magnification). Wound-healing assay results are quantified in the histogram. (D) Wound-healing assay results of A2780 cells are quantified in the histogram. (E) Western blotting analysis of the expression of EMT-related markers in SKOV3 cells. Scale bar, 50 μm . $n = 4-8$; * $p < 0.05$ and ** $p < 0.01$.

miR-101 Inhibits EMT and Cell Migration in OvCa Cell Lines by Directly Targeting FN1

To examine the effect of miR-101 on OvCa cells, we transfected miR-101 and miR-negative control (NC) into SKOV3 and A2780 cells. Data from Transwell assays showed that transient introduction of miR-101 into SKOV3 and A2780 cells inhibited migration in SKOV3 and A2780 cells and invasion in SKOV3 cells (Figures 2A and 2B). A wound-healing assay further confirmed that miR-101 inhibited cell migration (Figures 2C and 2D). Moreover, transfection with miR-101 resulted in disturbing expression of several EMT-related markers, including an increase in E-cadherin and a decrease in vimentin expression in SKOV3 cells (Figure 2E).

miRNAs are a class of small non-coding RNAs that essentially regulate gene expression via post-transcriptional regulation of mRNA.²⁵ Furthermore, FN1 and hsa-miR-101 expression were negatively correlated in OvCa (Figure 1E). FN1 has been reported to be involved in the development of multiple cancer types.²⁶ Evidence has suggested that FN1 can suppress apoptosis and promote cell invasion and migration in colorectal cancer, and SOX2 targets FN1 to promote cell migration and invasion in OvCa.^{21,27} However, there is no evidence of miRNAs targeting FN1 to regulate OvCa cell metastasis. As depicted in Figure 3A, using the TargetScan database (http://www.targetscan.org/vert_72/), we found that miR-101 had a complementary seed sequence with a binding site on the 3' UTR of FN1. A luciferase assay showed that co-transfection with miR-101 and a luciferase reporter carrying a portion of the human FN1 3' UTR (FN1-wild-type [WT]) caused a significant decrease in luciferase activity compared with co-transfection with miR-NC (Figure 3B). However, the luciferase activity was efficiently reversed when the potential miR-101 binding site was mutated (FN1-Mut) (Figure 3B).

Then, we transfected SKOV3 and A2780 cells with 50 nM miR-101 mimic and found that miR-101 significantly inhibited FN1 protein expression (Figures 3C and 3D). Consistently, transfection of SKOV3 or A2780 cells with 50 nM AMO-101 increased the protein expression levels of FN1 (Figures 3E and 3F). Moreover, real-time RT-PCR results showed that transfection of SKOV3 cells with miR-101 inhibited FN1 mRNA expression, whereas transfection with AMO-101 showed the opposite effects (Figures 3G and 3H). All the above results indicate that miR-101 contributes to EMT induction and OvCa cell metastasis by directly targeting FN1.

lncRNA PTAL Inhibits the Expression and Activity of miR-101 by Acting as a miRNA Sponge

lncRNAs may act as endogenous RNA sponges that interact with miRNAs and influence the expression and activity of the miRNAs.^{28,29} As shown in Figures 4A and 4B, ectopic expression of PTAL markedly reduced the miR-101 level in SKOV3 cells. In contrast, we applied small interfering RNA (siRNA) to silence the expression of PTAL (Figure 4C). siPTAL-2 was the most effective siRNA in knocking down PTAL, and the inhibition of PTAL dramatically enhanced the miR-101 expression level (Figures 4C and 4D).

Meanwhile, we constructed luciferase reporter vectors that contained wild-type or mutant miR-101 putative binding sites in PTAL. As shown in Figure 4E, the relative luciferase activity was suppressed in HEK293 cells co-transfected with miR-101 and PTAL-WT, whereas PTAL-Mut had no effect. Moreover, a miR-101 sensor reporter vector was constructed and showed an increase in luciferase activity in SKOV3 cells with PTAL transfection. These data indicate that miR-101 can attenuate the luciferase activity of the sensor, whereas PTAL decreases the inhibitory effects of miR-101 on its sensor (Figure 4F).

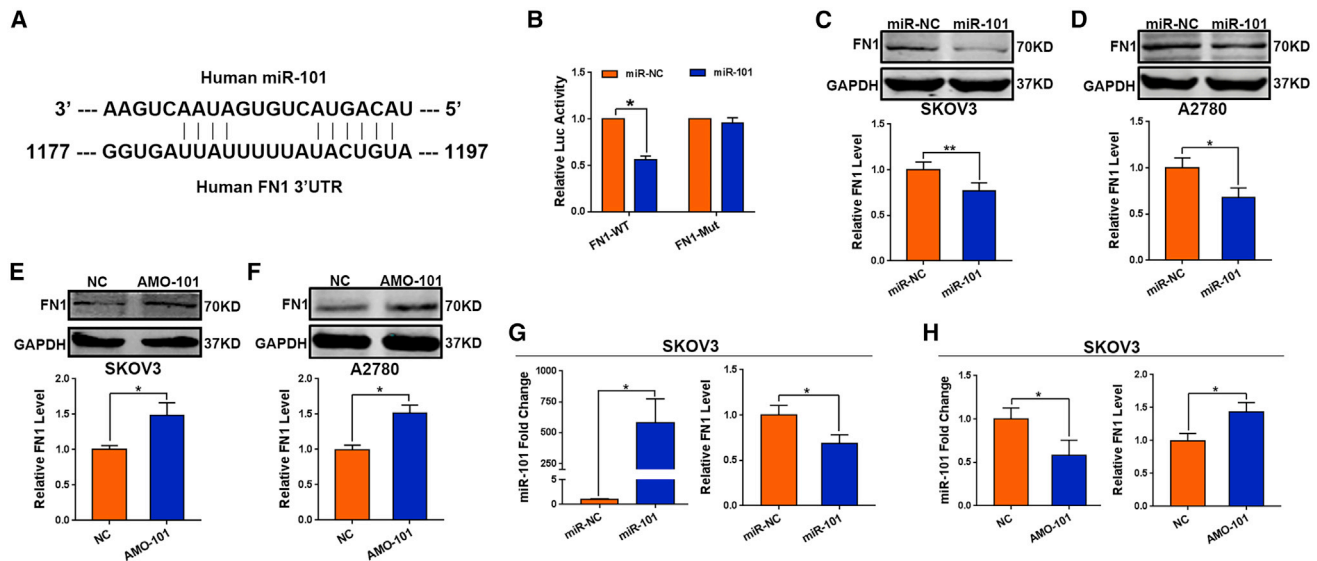


Figure 3. FN1 Is a Direct Target of miR-101

(A) Sequence alignment analysis revealed that miR-101 contains a complementary site for FN1. (B) The luciferase reporter activity of FN1-WT and FN1-Mut was detected in a luciferase assay. (C–F) Western blotting was used to determine the FN1 protein level in SKOV3 and A2780 cells after treatment with miR-101, miR-NC, AMO-101, or NC for 48 h. (C) Western blotting was used to determine the FN1 protein level in SKOV3 cells after treatment with miR-101 or miR-NC for 48 h. (D) Western blotting was used to determine the FN1 protein level in A2780 cells after treatment with miR-101 or miR-NC for 48 h. (E) Western blotting was used to determine the FN1 protein level in SKOV3 cells after treatment with AMO-101 or NC for 48 h. (F) Western blotting was used to determine the FN1 protein level in A2780 cells after treatment with AMO-101 or NC for 48 h. (G) Real-time RT-PCR analysis of the FN1 mRNA level in SKOV3 cells after treatment with miR-101 or miR-NC for 48 h. (H) Real-time RT-PCR analysis of the FN1 mRNA level in SKOV3 cells after treatment with AMO-101 or NC for 48 h. $n = 4-8$; * $p < 0.05$ and ** $p < 0.01$.

Furthermore, forced expression of PTAL increases the luciferase activity of the miR-101 sensor. In contrast, knockdown of PTAL has reverse effect (Figure 4G). Taken together, these results show that PTAL may directly regulate miR-101 expression and activity by binding to the putative binding sites and acting as a miRNA sponge. Furthermore, overexpression or silencing of PTAL upregulated or downregulated, respectively, the mRNA expression of FN1 (Figure 4H and 4I). All these data suggest that PTAL inhibits the expression and activity of miR-101 by acting as a miRNA sponge and regulates the expression of FN1 by competitively sponging miR-101. Thus, PTAL may be involved in regulation of the OvCa EMT program and cell invasion and migration, which is mediated by a miR-101-FN1 axis.

Overexpression of PTAL Promotes EMT and Metastasis of OvCa Cells by Regulating miR-101

Given that PTAL is highly expressed in the iM subtype of OvCa samples, we first validated the potential regulatory effects of PTAL overexpression on EMT and cancer cell migration and invasion. Transwell assays showed that overexpression of PTAL markedly enhanced the cell migration and invasion capability in both SKOV3 and A2780 cells (Figures 5A and 5B). Then, we tested the autonomous migratory ability of the cells using wound-healing assays. As shown in Figures 5C and 5D, forced expression of PTAL significantly accelerated the speed of wound closure in both SKOV3 and A2780 cells. To confirm that the functions of PTAL were indeed due to regulation of miR-101, we simultaneously trans-

fect SKOV3 and A2780 cells with PTAL and miR-101 mimics. The results showed that the miR-101 mimic reversed the invasion and migration abilities of SKOV3 and A2780 cells induced by PTAL overexpression (Figures 5A–5D).

Because EMT is a pivotal step necessary for epithelial cells to gain the ability to invade and metastasize, we tested the expression of EMT-related markers via western blotting and real-time RT-PCR. As shown in Figures 5E–5G, overexpression of PTAL resulted in downregulation of E-cadherin and Zo-1 but upregulation of N-cadherin, vimentin, and slug in SKOV3 and A2780 cells at the protein level and in SKOV3 cells at the mRNA level, indicating that overexpression of PTAL could induce the SKOV3 or A2780 cells to convert into mesenchymal cells, whereas miR-101 mimic reversed all those effects (Figures 5E–5G). Furthermore, PTAL upregulated the protein level of FN1 in SKOV3 and A2780 cells and the mRNA level of FN1 in SKOV3 cells, whereas miR-101 reversed these effects (Figures 5E–5G).

To further confirm whether miR-101 is necessary for PTAL activity in OvCa cells, a miR-101 inhibitor (AMO-101) or inhibitor NC were introduced into SKOV3 and A2780 cells. As depicted in Figures 6A–6D, co-transfection with AMO-101 abated the protective effects of siPTAL on the TGF- β 1-induced motility of SKOV3 and A2780 cells, which was evidenced by increased cell migration and invasion (Figures 6A and 6B) and the closed wound area (Figures 6C and 6D). Similarly, co-transfection with AMO-101 attenuated the

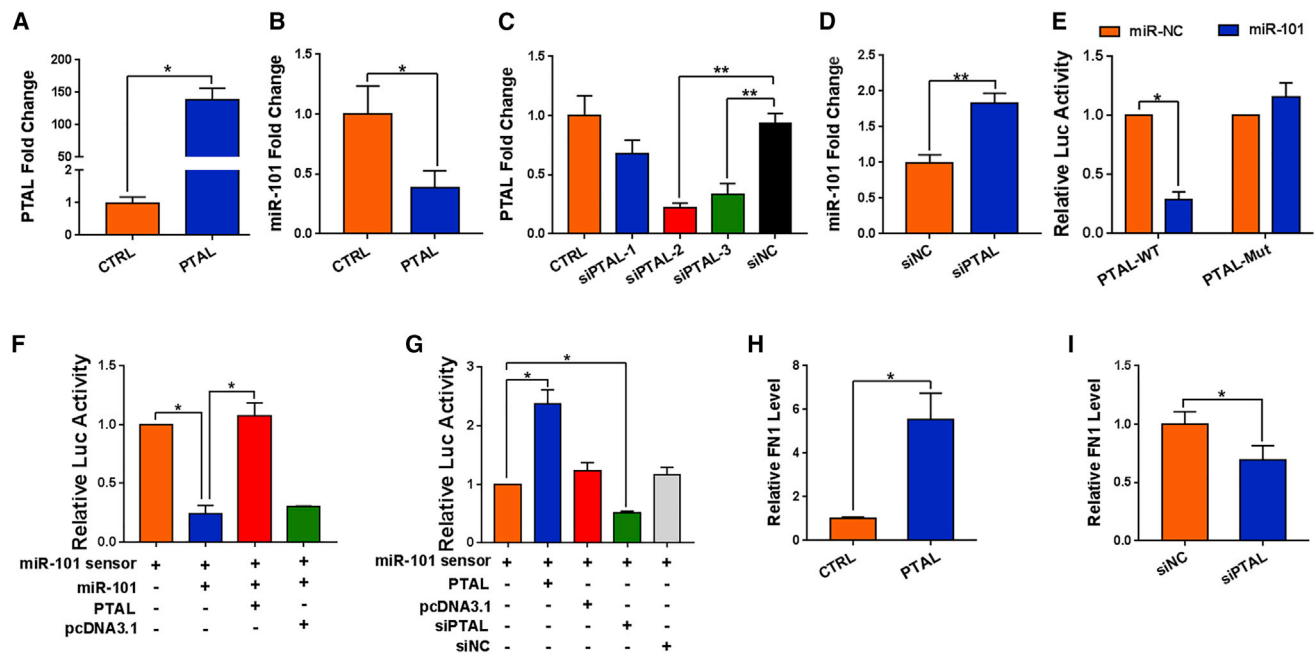


Figure 4. The lncRNA PTAL Acts as a miRNA Sponge of miR-101

(A) Real-time RT-PCR analysis of PTAL expression levels in SKOV3 cells transfected with PTAL plasmid. $n = 4$; $*p < 0.05$. (B) Real-time RT-PCR analysis of miR-101 expression levels in SKOV3 cells transfected with PTAL plasmid. $n = 8$; $*p < 0.05$. (C) Real-time RT-PCR analysis of PTAL expression levels in SKOV3 cells transfected with siPTAL for 48 h. $n = 4$; $**p < 0.01$. (D) Real-time RT-PCR analysis of miR-101 expression levels in SKOV3 cells transfected with siPTAL for 48 h. $n = 8$; $**p < 0.01$. (E) A luciferase activity assay was employed to analyze the luciferase activity in HEK293 cells co-transfected with PTAL-WT or PTAL-Mut and miR-101 or miR-NC. $n = 3$; $*p < 0.05$. (F) Luciferase activity of a miR-101 sensor in OvCa cells transfected with miR-101 sensor, miR-101 or PTAL as specified. $n = 3$; $*p < 0.05$. (G) Luciferase activity of a miR-101 sensor in OvCa cells transfected with miR-101 sensor, PTAL or siPTAL as specified. $n = 3$; $*p < 0.05$. (H) The FN1 mRNA level was detected in OvCa cells in response to overexpression of PTAL. (I) The FN1 mRNA level was detected in OvCa cells in response to silencing of PTAL. $n = 3$; $*p < 0.05$.

inhibitory effect of siPTAL on the EMT program in TGF- β 1-treated SKOV3 and A2780 cells, which was indicated by the protein and mRNA expression level of EMT markers (Figures 6E–6G). Simultaneously, silencing PTAL decreased the protein and mRNA level of FN1 in TGF- β 1-treated SKOV3 cells, but AMO-101 alleviated these effects (Figure 6E–6G). Taken together, these data suggest that silencing of PTAL protected against EMT and OvCa cell metastasis through the miR-101-FN1 axis.

Inhibition of PTAL Attenuated OvCa Tumorigenesis and Metastasis *In Vivo*

Considering the above results, we aimed to determine whether inhibition of PTAL displays protective effects on OvCa tumorigenesis and metastasis by employing a nude mouse xenograft tumor model. The nude mice were intraperitoneally injected with SKOV3 cells for 7 days, and then the mice were intraperitoneally injected with lentiviral constructs carrying short hairpin RNA (shRNA) against PTAL (shPTAL) or shScramble for 3 weeks. Significantly, the mice injected with shPTAL developed smaller tumors (Figure 7A) and had a decreased metastatic burden (Figure 7B) compared with mice in the shScramble group, but the treatments had no significant effects on mouse weight (Figure 7C). Western blotting and immunohistochemistry (IHC) were used to test the expression of EMT-related markers.

As depicted in Figure 7D, the tumors derived from mice injected with shPTAL exhibited an increased expression of Zo-1 and E-cadherin but decreased vimentin and Slug expression. Consistently, PTAL knockdown resulted in prominent, increased E-cadherin staining, as well as less-intense FN1 and vimentin staining, compared with the staining in tumor tissues from the shScramble group (Figure 7E). These data indicate that silencing of PTAL inhibits ovarian tumorigenesis and metastasis *in vivo*.

DISCUSSION

In the present study, we reveal that PTAL plays an important role in EMT progression and OvCa metastasis. Given the evidence from *in vivo* and *in vitro* experiments, we made a hypothesis model in iE OvCa samples and in iM OvCa samples. As shown in Figure 7F, miR-101 is highly expressed in integrated epithelial (iE) OvCa samples where PTAL expression is low, and miR-101 maintains epithelium characteristics of cells by inhibiting FN1 transcription. However, in iM OvCa samples, high expression of PTAL leads to increased expression of FN1 through competitive binding of miR-101, and thus, PTAL acts as a miRNA sponge and promotes OvCa cell EMT and metastasis. Our findings not only reveal a positive correlation between PTAL and FN1 and a negative correlation between miR-101 and PTAL and FN1 but also provide a new possible target for preventing OvCa metastasis

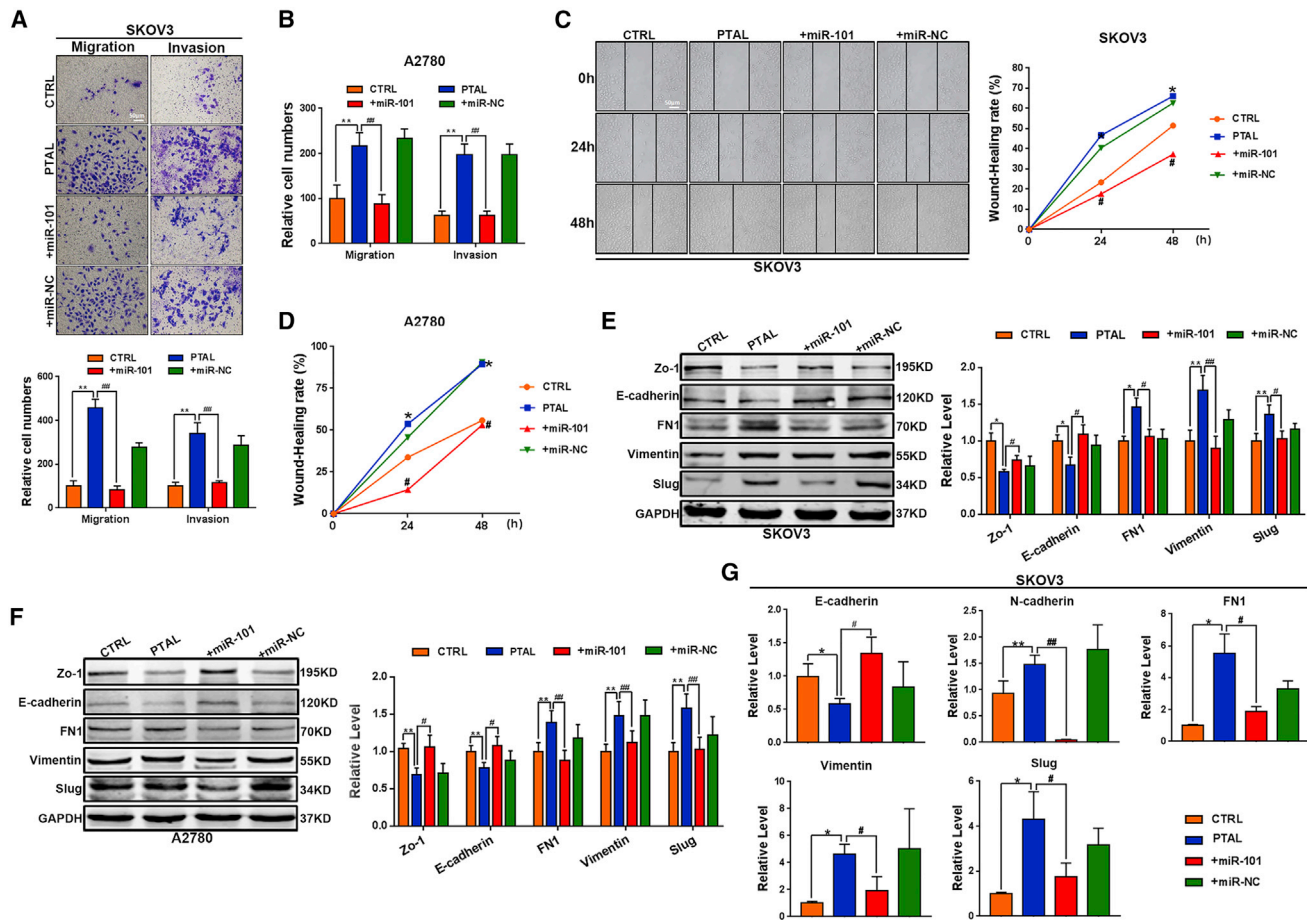


Figure 5. Effects of PTAL on Invasion and Migration of OvCa Cells In Vitro

SKOV3 and A2780 cells were transfected with PTAL plasmid with or without miR-101 for 48 h. (A) Representative images of the migration and invasion of SKOV3 cells. Cells were counted for the corresponding assays in at least four random microscope fields ($\times 100$ magnification). Cell migration and invasion are expressed as a percentage of the control cell values. (B) The migration and invasion ability of A2780 cells were determined with Transwell assays. (C) Representative images from wound-healing assays of SKOV3 cells ($\times 100$ magnification). The wound-healing assay results are quantified in the histogram. (D) The wound-healing assay results are quantified in the histogram. Western blotting (E for SKOV3 cells), western blotting (F for A2780 cells), and real-time RT-PCR analysis (G) showing the protein levels of EMT-related markers in SKOV3 and A2780 cells and the mRNA levels of EMT-related markers in SKOV3 cells. Scale bar, 50 μ m. $n = 4-10$; * $p < 0.05$, ** $p < 0.01$ versus CTRL; # $p < 0.05$, ## $p < 0.01$ versus PTAL.

by showing the importance of the PTAL-miR-101-FN1 axis in regulating OvCa EMT and the invasion-metastasis cascade.

lncRNAs have been suggested to play oncogenic or tumor-suppressor roles in many different cancers and biological functions through their interactions with other cellular macromolecules, such as chromatin DNA, RNA, or protein. EPIC1 is an oncogenic lncRNA that interacts with Myc and promotes cell cycle progression in breast cancer.³⁰ TTN-AS1, another oncogenic lncRNA, promotes esophageal squamous cell carcinoma proliferation and metastasis by promoting expression of the transcription factor Snail1 by competitively binding miR-133b, resulting in EMT.²⁶ Decreased expression of the lncRNA FENRR is associated with poor prognosis in gastric cancer, and FENRR suppresses gastric cancer cell metastasis by inhibiting FN1 expression.³¹ The lncRNA HOXA11-AS promotes proliferation

and invasion of gastric cancer by scaffolding the chromatin modification factors PRC2, LSD1, and DNMT1.³² Thus, our study reveals how PTAL exerts its function in promoting OvCa invasion and migration.

To explore the molecular mechanism by which PTAL promoted invasion and metastasis in OvCa, we investigated potential targets involved in cell motility and matrix invasion through a bioinformatics analysis. The results revealed that the expression of PTAL and miR-101 were correlated in iM OvCa samples. Some studies have reported that miR-101 plays an important role in cancer metastasis by targeting different downstream genes, including ZEB1, EZH2, and PIM1.^{18,33-35} However, there is a limited understanding of the roles of miR-101 in OvCa. We found that the expression of miR-101, which was reduced or elevated after overexpression or blocking of PTAL, respectively, was downregulated in OvCa samples. In this study, we

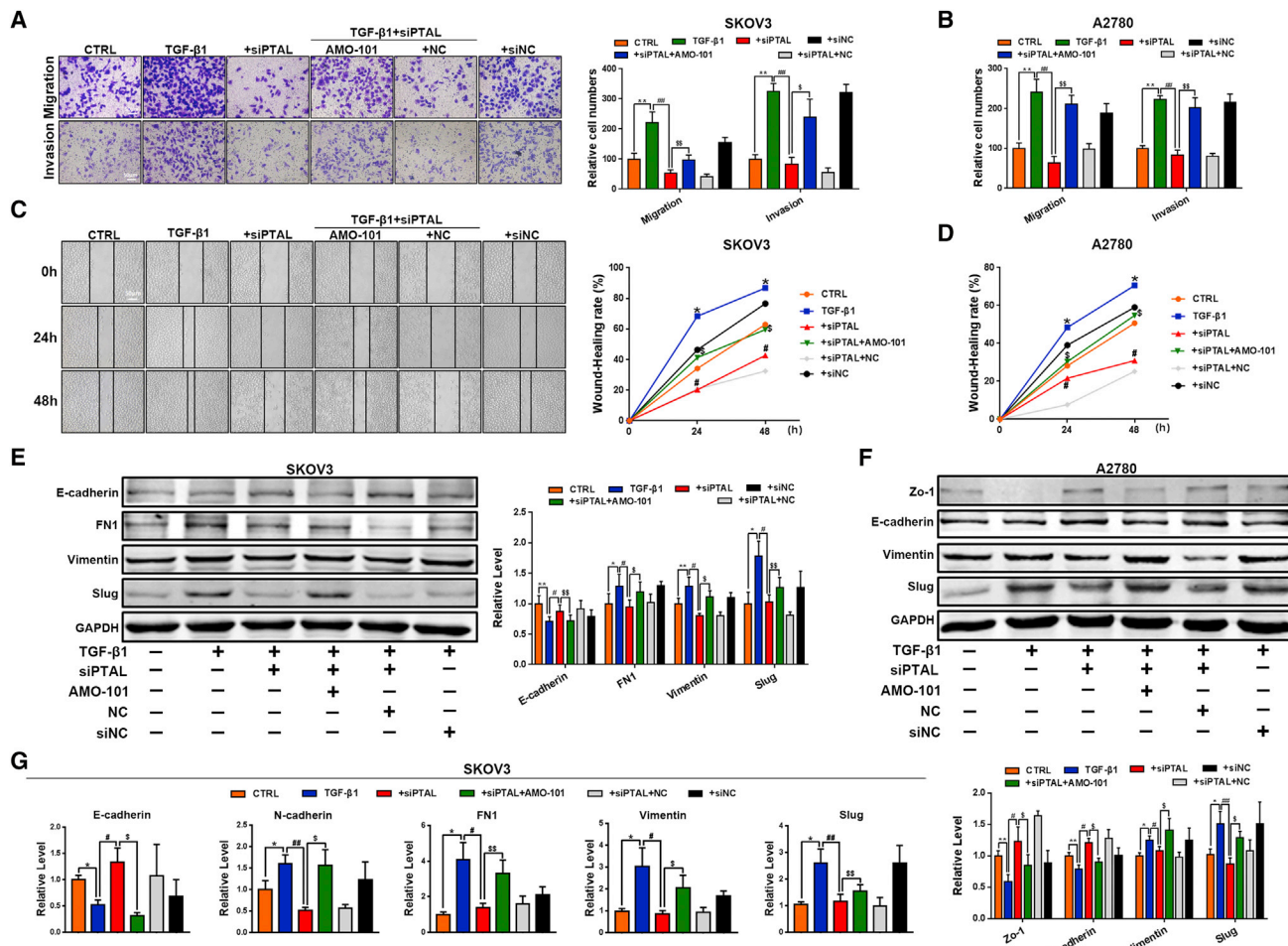


Figure 6. Silencing of PTAL Suppresses Invasion and Migration of OvCa Cells

SKOV3 and A2780 cells were transfected with siRNA against PTAL with or without miR-101 inhibitor in the presence or absence of 10 ng/mL TGF- β 1 for 48 h. (A) Representative images of the migration and invasion of SKOV3 cells. Cells were counted for the corresponding assays in at least four random microscope fields ($\times 100$ magnification). Cell migration and invasion are expressed as a percentage of the control cell values. (B) The migration and invasion ability of A2780 cells was determined with Transwell assays. (C) Representative images from wound-healing assays of SKOV3 cells ($\times 100$ magnification). The wound-healing assay results are quantified in the histogram (right panel). (D) The wound-healing assay results of A2780 cells are quantified in the histogram. Western blotting (E for SKOV3 cells), western blotting (F for A2780 cells), and real-time RT-PCR analysis (G) showing the protein levels of EMT-related markers in SKOV3 and A2780 cells and the mRNA levels of EMT-related markers in SKOV3 cells. Scale bar, 50 μ m. $n = 4-10$; * $p < 0.05$ and ** $p < 0.01$ versus CTRL; # $p < 0.05$ and ## $p < 0.01$ versus TGF- β 1; $\$p < 0.05$ and \$\$ $p < 0.01$ versus TGF- β 1+siPTAL.

demonstrate that PTAL acts as an endogenous RNA sponge that interacts with miR-101 and affects the expression and function of miR-101.

Finally, to explore the molecular mechanism by which miR-101 contributed to invasion and metastasis in OvCa, we predicted the potential targets of miR-101 using the TargetScan database.³⁶ Among the predicted targets of miR-101, FN1 showed significant upregulation in iM OvCa samples and had a significant negative correlation with miR-101 expression. FN1, an extracellular matrix glycoprotein, plays major roles in cell adhesion, migration, and differentiation.³⁷ Importantly, FN1 is also the key mediator of carcinomagenesis and tumor metastasis, including in lung adenocarcinoma, gastric

cancer, and brain glioblastoma.^{31,38,39} It has been reported that FN1 mediates glioma progression by interacting with integrin β ³⁸, and FN1 can activate MMP2/MMP9 to promote invasion and migration in multiple carcinoma types.^{38,40} However, the precise molecular mechanism underlying FN1 regulation of OvCa metastasis remains unclear and requires further investigation. In this study, we found that FN1 is a direct target of miR-101, and its mRNA and protein levels were elevated or reduced after transfection with miR-101 or AMO-101. Moreover, IHC analysis showed that the FN1 protein level in tissues from a xenograft model with injected shPTAL was lower than in tissues from the control group. Our results confirmed that FN1 might be negatively regulated by miR-101 and positively regulated by PTAL.

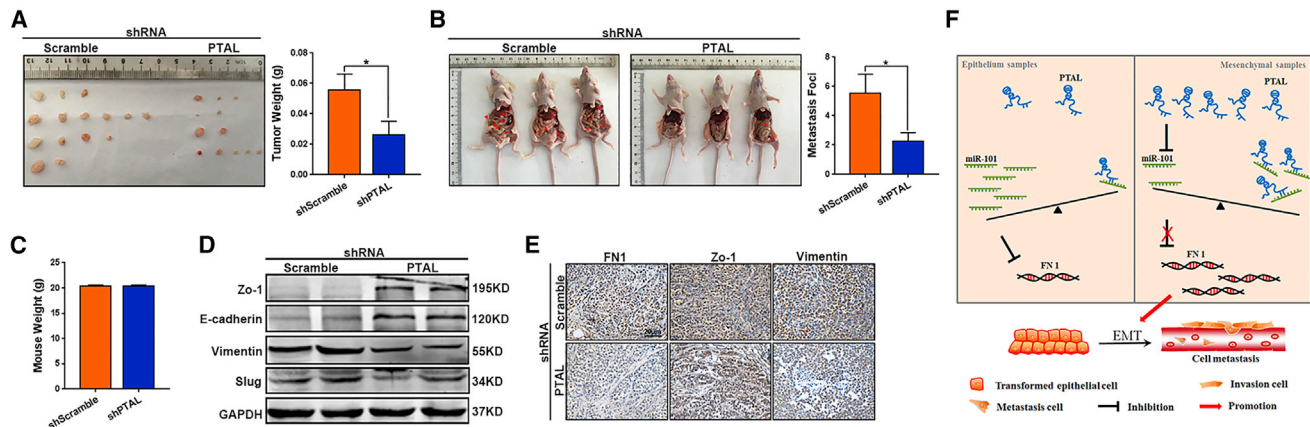


Figure 7. Knockdown of PTAL Inhibits Ovarian Tumorigenesis and Metastasis in a Xenograft Model

(A) Tumors collected from mice are presented. Tumor weights from mice were measured and analyzed. shScramble, n = 9; shPTAL, n = 12. *p < 0.05. (B) Visualization of the entire abdominal cavity with the number of tumor nodules on the intestinal surfaces. The metastatic foci were analyzed. shScramble, n = 9; shPTAL, n = 12; *p < 0.05. (C) The mouse weights were measured and analyzed. shScramble, n = 9; shPTAL, n = 12. (D) Western blotting was used to analyze the expression of EMT-related markers in tumor tissues from the shScramble and shPTAL groups. (E) Representative images of immunohistochemistry (IHC) staining of FN1, Zo-1, and vimentin in xenograft tumor tissues from nude mice; scale bar, 20 μ m. n = 3. (F) Model of the role of PTAL and miR-101 in OvCa progression.

In our previous work, we demonstrated that lncRNA PTAR promoted EMT and invasion metastasis in OvCa by competitively binding miR-101 to regulate ZEB1 expression.²⁰ Upregulation of PTAR led to elevated expression of ZEB1 through competitive binding of PTAR to miR-101 as a ceRNA of miR-101, which promoted OvCa EMT and metastasis.²⁰ Both ZEB1 and FN1 are key genes involved in the EMT process. Our studies reveals that both ZEB1 and FN1 are targets of miR-101, which highlights the key roles of miR-101 in the EMT process. More importantly, we reveal that the lncRNAs PTAR and PTAL can promote the EMT process in OvCa cells by regulating miR-101. Thus, the lncRNAs PTAR and PTAL may cooperatively regulate miR-101, which is involved in the OvCa invasion and metastasis. The PTAL-miR-101-FN1 and PTAR-miR-101-ZEB1 axis may form a cooperative network to regulate the EMT process during OvCa metastasis, which warrants further detailed study.

In summary, our study showed that upregulation of PTAL played a positive role in OvCa metastasis and revealed that PTAL positively regulated the expression of FN1 through sponging of miR-101, which promoted OvCa cell invasion and migration. These findings shed new light on lncRNA-directed therapeutics for preventing OvCa metastasis.

MATERIALS AND METHODS

Cell Culture, Reagents, and Expression Constructs

The OvCa cell lines A2780 and SKOV3 were purchased from the Cell Bank of the Chinese Academy of Sciences (Shanghai, China). Cells were cultured in RPMI 1640 (Gibco, NY, USA) or DMEM (Gibco, NY, USA) supplemented with 10% fetal bovine serum (FBS; Biological Industries) and 1% penicillin/streptomycin at 37°C and 5% CO₂. Expression plasmids encoding PTAL were constructed using pcDNA3.1. All plasmids were isolated using an

EasyPure HiPure plasmid maxiprep kit (TransGen Biotech, Shanghai, China). An hsa-miR-101 mimic was used in place of miR-101 expression. A chemically modified antisense oligonucleotide (antagomir AMO-101) was used to inhibit miR-101 expression, and a scramble oligonucleotide was used as the NC (miR-NC for miR-101, NC for AMO-101). The miR-101 mimic, inhibitor, and stable NC were purchased from GenePharma (Shanghai, China). For transfection, cells were cultured in 6-well plates until they reached 70%–80% confluence. The cells were then transfected with plasmids using Lipofectamine 2000 (Invitrogen, Carlsbad, CA, USA) based on the manufacturer's instructions. Six hours after transfection of lncRNA or luciferase vector, cholesterol-modified miR-101 mimic or inhibitor was added and incubated with the cells for 48 h.

Wound-Healing and Transwell Assays

For wound-healing assays, cells were seeded at a density of 1×10^6 cells/well in 6-well plates. An artificial wound was created on a confluent cell monolayer 6 h after transfection using a sterile 10- μ L pipette tip. The non-adhered cells were washed away with PBS, and the cells were then cultured in medium with 2% FBS (Biological Industries, Cromwell, CT, USA). The wounds were photographed with a light microscope at 0, 24, and 48 h after treatment. *In vitro* cell migration and invasion were investigated using a 24-well Transwell insert without (migration assay) or with (invasion assay) Matrigel (8.0 μ m, Corning, NY, USA). For the migration assay, 5×10^4 cells were suspended in 200 μ L of serum-free DMEM or RPIM 1640 (Gibco, Life Technologies, Carlsbad, CA, USA) and placed in the top chambers. For the invasion assay, 2×10^5 cells were suspended in 200 μ L of DMEM or RPIM 1640 without serum and then seeded on the cell culture insert precoated with 1 μ g/ μ L Matrigel. Complete medium was added to the bottom wells to stimulate migration or invasion. After incubation for 48 h, the cells that did not penetrate

through the membrane were removed with a cotton swab, while those adhered to the lower surface of the membrane were stained with 0.1% crystal violet solution. The number of migrated cells in five randomly selected fields was determined under a light microscope (Olympus, Tokyo, Japan).

Immunohistochemistry Assay

In brief, immunostaining was performed on 5- μ m-thick tissue sections. The sections were dewaxed, deparaffinized in xylene, and rehydrated in graded alcohol solutions. The antigen-retrieval process was performed by heating the sections for 30 min in Tris-EDTA buffer. The slides were subsequently stained with primary antibodies for E-cadherin (Cell Signaling, #9562, MA, USA; 1:100) and vimentin (Cell Signaling, #5741, MA, USA; 1:100) and their respective secondary antibodies. The sections were then counterstained with hematoxylin, followed by dehydration and mounting. Images were captured with an Olympus camera.

Lentiviral Vector Construct and Xenograft Model in Nude Mice

The constructs of PTAL shRNA packaged with lentivirus were constructed by Biowit Technology (Shenzhen, China). Female BALB/c nude mice (5 weeks old) were purchased from Beijing Vital River Laboratory Animal Technology (Beijing, China) and maintained in pathogen-free conditions. The nude mice were infected with the constructed vectors packaged with lentivirus at day 7 following tumor xenografts. To form xenografts, 10⁶ SKOV3 cells were intraperitoneally injected into female BALB/c nude mice. The nude mice were housed under specific pathogen-free conditions and sacrificed after 28 days. Then, the xenograft tumor tissues were harvested, weighed, formalin-fixed, and paraffin-embedded for subsequent immunohistochemistry staining. The remaining tumor tissues were stored at -80°C for analysis of protein and RNA levels. The procedures were performed in accordance with the regulations of the Ethics Committee of Harbin Medical University and the Guide for the Care and Use of Laboratory Animals published by the National Institutes of Health (NIH publication no. 85-23, 2011).

RNA Preparation and Real-Time RT-PCR

Total RNA was isolated from cultured cells using Trizol reagent (Invitrogen, Carlsbad, CA, USA) according to the manufacturer's instructions. RNA integrity, quantity, and purity were examined using a Nano-Drop 8000 spectrophotometer (Thermo Scientific, Wilmington, DE, USA). As delineated in our previous work, cDNA was generated using a high-capacity cDNA reverse transcription kit (Applied Biosystems, Foster City, CA, USA). Real-time PCR was performed on an ABI7500 FAST real-time PCR system (Applied Biosystems) for 40 cycles. After the reaction cycles, the threshold cycle (Ct) values were determined, and the relative mRNA levels were calculated based on the Ct values and normalized to the GAPDH or U6 level in each sample. Primer sets for PTAL, miR-101, FN1, vimentin, E-cadherin, N-cadherin, and Slug were purchased from Invitrogen (Shanghai, China). The primer sequence of PTAL was as follows: forward, 5'-CTGCATACCACTTTAAAGAGCC-3'; reverse, 5'-AGGCAGCGCTTGACAGTGAGC-3'. The primer sequence of miR-101 RT was

as follows: 5'-GTCGTATCCAGTGC GTGTCTGTTGGAGTCGGCA ATTGCACTGGATACGACTtcagtta-3'; forward, 5'-GCGG tacagttgtga-3'; reverse, 5'-TGTCGTGGAGTCGGCAATTG-3'. The expression levels of GAPDH or U6 were used as internal controls; U6 was used for mRNA transcripts. Fold changes in the expression of mRNA among the RNA samples were calculated.

Western Blotting and Antibodies

For western blot analyses, total protein was extracted from the cells. Approximately 40 μ g of crude protein was denatured and electrophoresed on 10% SDS-PAGE gels. After electrophoretic separation, proteins were transferred onto nitrocellulose membranes (Merck Millipore, R7BA46025) by electroblotting and then blocked for 70 min at room temperature in PBS containing 5% non-fat milk; the blots were probed with primary antibodies, and GAPDH was used as the internal control. The blots were incubated with primary antibodies targeting FN1 (Proteintech, 15613-1-AP, Wuhan, China; 1:400), Slug (Cell Signaling, #9585, MA, USA; 1:300), E-cadherin (Cell Signaling, #9562, MA, USA; 1:1,000), vimentin (Cell Signaling, #5741, MA, USA; 1:1,000), Zo-1 (Proteintech, 21773-1-AP, Wuhan, China; 1:500), and GAPDH (ABclonal, AC002, Wuhan, China; 1:1,000) in PBS at 4°C overnight. The membranes were washed with PBS+Tween20 (PBS-T) and then incubated with secondary antibody (Alexa Fluor) for 1 h at room temperature. Finally, images of the western blot bands were collected with an imaging system (Odyssey, LI-COR, USA) and quantified by measuring the intensity in each group using Odyssey v1.2 software; GAPDH was used as the internal control. The results are expressed as fold changes, and the data are normalized to the control values.

Statistical Analysis

All data analyses in this study were carried out using GraphPad Prism 7 software (GraphPad Software). Quantifications were performed using at least three independent experimental groups. When only two groups were compared, statistical analyses between groups were performed using two-tailed Student's t tests to determine significance. p values of less than 0.05 were considered significant. Error bars on all graphs represent the SEM unless otherwise indicated.

AUTHOR CONTRIBUTIONS

Y.G. and H.L. designed the project; M.Y., Lu Zhang, Y.H., D.Z., and J.S. performed cell experiments; R.Y., Lijia Zhang, T.Y., and H.L. conducted animal experiments; Y.G. and H.S. performed bioinformatics analysis; M.Y., Y.G., and H.L. wrote the manuscript.

CONFLICTS OF INTERESTS

The authors declare no competing interests.

ACKNOWLEDGMENTS

This study was supported by the National Natural Science Foundation of China (61673143 and 31671187), the Postdoctoral Scientific Research Developmental Fund (LBH-Q16166), and the University Nursing Program for Young Scholars with Creative Talents in Heilongjiang Province (UNPYSCT-2017061).

REFERENCES

- Cannistra, S.A. (2004). Cancer of the ovary. *N. Engl. J. Med.* 351, 2519–2529.
- Yang, D., Sun, Y., Hu, L., Zheng, H., Ji, P., Pecot, C.V., Zhao, Y., Reynolds, S., Cheng, H., Rupaimoole, R., et al. (2013). Integrated analyses identify a master microRNA regulatory network for the mesenchymal subtype in serous ovarian cancer. *Cancer Cell* 23, 186–199.
- Cao, L., Shao, M., Schilder, J., Guise, T., Mohammad, K.S., and Matei, D. (2012). Tissue transglutaminase links TGF- β , epithelial to mesenchymal transition and a stem cell phenotype in ovarian cancer. *Oncogene* 31, 2521–2534.
- Agarwal, R., and Kaye, S.B. (2003). Ovarian cancer: strategies for overcoming resistance to chemotherapy. *Nat. Rev. Cancer* 3, 502–516.
- Ciommella, P., Luminari, S., Arcaini, L., and Filippi, A.R. (2018). Renewed interest for low-dose radiation therapy in follicular lymphomas: From biology to clinical applications. *Hematol. Oncol.* 36, 723–732.
- Liu, B., Sun, L., Liu, Q., Gong, C., Yao, Y., Lv, X., Lin, L., Yao, H., Su, F., Li, D., et al. (2015). A cytoplasmic NF- κ B interacting long noncoding RNA blocks I κ B phosphorylation and suppresses breast cancer metastasis. *Cancer Cell* 27, 370–381.
- Zhao, Z., Zhou, W., Han, Y., Peng, F., Wang, R., Yu, R., Wang, C., Liang, H., Guo, Z., and Gu, Y. (2017). EMT-Regulome: a database for EMT-related regulatory interactions, motifs and network. *Cell Death Dis.* 8, e2872.
- Zhang, X.Q., Sun, S., Lam, K.F., Kiang, K.M., Pu, J.K., Ho, A.S., Lui, W.M., Fung, C.F., Wong, T.S., and Leung, G.K. (2013). A long non-coding RNA signature in glioblastoma multiforme predicts survival. *Neurobiol. Dis.* 58, 123–131.
- Chen, J., Wang, R., Zhang, K., and Chen, L.B. (2014). Long non-coding RNAs in non-small cell lung cancer as biomarkers and therapeutic targets. *J. Cell. Mol. Med.* 18, 2425–2436.
- Wang, Z., Yang, B., Zhang, M., Guo, W., Wu, Z., Wang, Y., Jia, L., and Li, S.; Cancer Genome Atlas Research Network (2018). lncRNA Epigenetic Landscape Analysis Identifies EPIC1 as an Oncogenic lncRNA that Interacts with MYC and Promotes Cell-Cycle Progression in Cancer. *Cancer Cell* 33, 706–720.e9.
- Wu, D.D., Chen, X., Sun, K.X., Wang, L.L., Chen, S., and Zhao, Y. (2017). Role of the lncRNA ABHD11-AS₁ in the tumorigenesis and progression of epithelial ovarian cancer through targeted regulation of RhoC. *Mol. Cancer* 16, 138.
- Huarte, M. (2015). The emerging role of lncRNAs in cancer. *Nat. Med.* 21, 1253–1261.
- Wang, X., Yu, H., Sun, W., Kong, J., Zhang, L., Tang, J., Wang, J., Xu, E., Lai, M., and Zhang, H. (2018). The long non-coding RNA CYTOR drives colorectal cancer progression by interacting with NCL and Sam68. *Mol. Cancer* 17, 110.
- Liang, H., Zhao, X., Wang, C., Sun, J., Chen, Y., Wang, G., Fang, L., Yang, R., Yu, M., Gu, Y., and Shan, H. (2018). Systematic analyses reveal long non-coding RNA (PTAF)-mediated promotion of EMT and invasion-metastasis in serous ovarian cancer. *Mol. Cancer* 17, 96.
- Ye, Z., Zhou, M., Tian, B., Wu, B., and Li, J. (2015). Expression of lncRNA-CCAT1, E-cadherin and N-cadherin in colorectal cancer and its clinical significance. *Int. J. Clin. Exp. Med.* 8, 3707–3715.
- Grelet, S., Link, L.A., Howley, B., Obellianne, C., Palanisamy, V., Gangaraju, V.K., Diehl, J.A., and Howe, P.H. (2017). A regulated PNUTS mRNA to lncRNA splice switch mediates EMT and tumour progression. *Nat. Cell Biol.* 19, 1105–1115.
- Terashima, M., Tange, S., Ishimura, A., and Suzuki, T. (2017). MEG3 Long Noncoding RNA Contributes to the Epigenetic Regulation of Epithelial-Mesenchymal Transition in Lung Cancer Cell Lines. *J. Biol. Chem.* 292, 82–99.
- Liu, D., Li, Y., Luo, G., Xiao, X., Tao, D., Wu, X., Wang, M., Huang, C., Wang, L., Zeng, F., and Jiang, G. (2017). lncRNA SPRY4-IT1 sponges miR-101-3p to promote proliferation and metastasis of bladder cancer cells through up-regulating EZH2. *Cancer Lett.* 388, 281–291.
- Cao, K., Li, J., Zhao, Y., Wang, Q., Zeng, Q., He, S., Yu, L., Zhou, J., and Cao, P. (2016). miR-101 Inhibiting Cell Proliferation, Migration and Invasion in Hepatocellular Carcinoma through Downregulating Girdin. *Mol. Cells* 39, 96–102.
- Liang, H., Yu, T., Han, Y., Jiang, H., Wang, C., You, T., Zhao, X., Shan, H., Yang, R., Yang, L., et al. (2018). lncRNA PTAR promotes EMT and invasion-metastasis in serous ovarian cancer by competitively binding miR-101-3p to regulate ZEB1 expression. *Mol. Cancer* 17, 119.
- Cai, X., Liu, C., Zhang, T.N., Zhu, Y.W., Dong, X., and Xue, P. (2018). Down-regulation of FN1 inhibits colorectal carcinogenesis by suppressing proliferation, migration, and invasion. *J. Cell. Biochem.* 119, 4717–4728.
- Liu, F., Cheng, Z., Li, X., Li, Y., Zhang, H., Li, J., Liu, F., Xu, H., and Li, F. (2017). A Novel Pak1/ATF2/miR-132 Signaling Axis Is Involved in the Hematogenous Metastasis of Gastric Cancer Cells. *Mol. Ther. Nucleic Acids* 8, 370–382.
- Na, Y., Kaul, S.C., Ryu, J., Lee, J.S., Ahn, H.M., Kaul, Z., Kalra, R.S., Li, L., Widodo, N., Yun, C.O., and Wadhwa, R. (2016). Stress chaperone mortalin contributes to epithelial-mesenchymal transition and cancer metastasis. *Cancer Res.* 76, 2754–2765.
- Guttman, M., and Rinn, J.L. (2012). Modular regulatory principles of large non-coding RNAs. *Nature* 482, 339–346.
- Iqbal, M.A., Arora, S., Prakasam, G., Calin, G.A., and Syed, M.A. (2019). MicroRNA in lung cancer: role, mechanisms, pathways and therapeutic relevance. *Mol. Aspects Med.* 70, 3–20.
- Xu, T.P., Huang, M.D., Xia, R., Liu, X.X., Sun, M., Yin, L., Chen, W.M., Han, L., Zhang, E.B., Kong, R., et al. (2014). Decreased expression of the long non-coding RNA FENRR is associated with poor prognosis in gastric cancer and FENRR regulates gastric cancer cell metastasis by affecting fibronectin1 expression. *J. Hematol. Oncol.* 7, 63.
- Lou, X., Han, X., Jin, C., Tian, W., Yu, W., Ding, D., Cheng, L., Huang, B., Jiang, H., and Lin, B. (2013). SOX2 targets fibronectin 1 to promote cell migration and invasion in ovarian cancer: new molecular leads for therapeutic intervention. *OMICS* 17, 510–518.
- Thomson, D.W., and Dinger, M.E. (2016). Endogenous microRNA sponges: evidence and controversy. *Nat. Rev. Genet.* 17, 272–283.
- Tay, Y., Rinn, J., and Pandolfi, P.P. (2014). The multilayered complexity of ceRNA crosstalk and competition. *Nature* 505, 344–352.
- Lin, C., Zhang, S., Wang, Y., Wang, Y., Nice, E., Guo, C., Zhang, E., Yu, L., Li, M., Liu, C., et al. (2018). Functional Role of a Novel Long Noncoding RNA TTN-AS1 in Esophageal Squamous Cell Carcinoma Progression and Metastasis. *Clin. Cancer Res.* 24, 486–498.
- Yan, K., Tian, J., Shi, W., Xia, H., and Zhu, Y. (2017). lncRNA SNHG6 is Associated with Poor Prognosis of Gastric Cancer and Promotes Cell Proliferation and EMT through Epigenetically Silencing p27 and Sponging miR-101-3p. *Cell. Physiol. Biochem.* 42, 999–1012.
- Liu, Z., Chen, Z., Fan, R., Jiang, B., Chen, X., Chen, Q., Nie, F., Lu, K., and Sun, M. (2017). Over-expressed long noncoding RNA HOXA11-AS promotes cell cycle progression and metastasis in gastric cancer. *Mol. Cancer* 16, 82.
- Xu, Y., Yao, Y., Jiang, X., Zhong, X., Wang, Z., Li, C., Kang, P., Leng, K., Ji, D., Li, Z., et al. (2018). SP1-induced upregulation of lncRNA SPRY4-IT1 exerts oncogenic properties by scaffolding EZH2/LSD1/DNMT1 and sponging miR-101-3p in cholangiocarcinoma. *J. Exp. Clin. Cancer Res.* 37, 81.
- Liu, X.Y., Liu, Z.J., He, H., Zhang, C., and Wang, Y.L. (2015). MicroRNA-101-3p suppresses cell proliferation, invasion and enhances chemotherapeutic sensitivity in salivary gland adenoid cystic carcinoma by targeting Pim-1. *Am. J. Cancer Res.* 5, 3015–3029.
- Pankov, R., and Yamada, K.M. (2002). Fibronectin at a glance. *J. Cell Sci.* 115, 3861–3863.
- Agarwal, V., Bell, G.W., Nam, J.W., and Bartel, D.P. (2015). Predicting effective microRNA target sites in mammalian mRNAs. *eLife* 4, <https://doi.org/10.7554/eLife.05005>.
- Ritzenthaler, J.D., Han, S., and Roman, J. (2008). Stimulation of lung carcinoma cell growth by fibronectin-integrin signalling. *Mol. Biosyst.* 4, 1160–1169.
- Chung, S., Nakagawa, H., Uemura, M., Piao, L., Ashikawa, K., Hosono, N., Takata, R., Akamatsu, S., Kawaguchi, T., Morizono, T., et al. (2011). Association of a novel long non-coding RNA in 8q24 with prostate cancer susceptibility. *Cancer Sci.* 102, 245–252.
- Sengupta, S., Nandi, S., Hindi, E.S., Wainwright, D.A., Han, Y., and Lesniak, M.S. (2010). Short hairpin RNA-mediated fibronectin knockdown delays tumor growth in a mouse glioma model. *Neoplasia* 12, 837–847.
- Sen, T., Dutta, A., Maity, G., and Chatterjee, A. (2010). Fibronectin induces matrix metalloproteinase-9 (MMP-9) in human laryngeal carcinoma cells by involving multiple signaling pathways. *Biochimie* 92, 1422–1434.